Living beyond the edge: Higgs inflation and vacuum metastability

Fedor Bezrukov,[1, 2, 3, *] Javier Rubio,[4, †] and Mikhail Shaposhnikov[4, ‡]

[1]*Physics Department, University of Connecticut, Storrs, CT 06269-3046, USA*
[2]*RIKEN-BNL Research Center, Brookhaven National Laboratory, Upton, NY 11973, USA*
[3]*CERN, CH-1211 Geneve 23, Switzerland*
[4]*Institut de Théorie des Phénomènes Physiques, École Polytechnique Fédérale de Lausanne, CH-1015 Lausanne, Switzerland*
(Dated: December 15, 2014)

The measurements of the Higgs mass and top Yukawa coupling indicate that we live in a very special Universe, at the edge of the absolute stability of the electroweak vacuum. If fully stable, the Standard Model (SM) can be extended all the way up to the inflationary scale and the Higgs field, non-minimally coupled to gravity with strength ξ, can be responsible for inflation. We show that the successful Higgs inflation scenario can also take place if the SM vacuum is not absolutely stable. This conclusion is based on two effects that were overlooked previously. The first one is associated with the effective renormalization of the SM couplings at the energy scale M_P/ξ, where M_P is the Planck scale. The second one is a symmetry restoration after inflation due to high temperature effects that leads to the (temporary) disappearance of the vacuum at Planck values of the Higgs field.

I. INTRODUCTION

One of the most interesting questions in particle physics and cosmology is the relation between the properties of elementary particles and the structure of the Universe. Some links are provided by Dark Matter and the Baryon Asymmetry of the Universe. A number of constraints on hypothetical new particles can be also derived from Big Bang Nucleosynthesis.

The properties of the recently discovered Higgs boson [1, 2] suggest an additional and intriguing connection. Among the many different values that the Higgs mass could have taken, Nature has chosen one that allows to extend the Standard Model (SM) all the way till the Planck scale while staying in the perturbative regime. The behavior of the Higgs self-coupling λ is quite peculiar: it decreases with energy to eventually arrive to a minimum at Planck scale values and start increasing thereafter, cf. Fig. 1. Within the experimental and theoretical uncertainties[1] the Higgs coupling may stay positive all way till the Planck scale, but it may also cross zero at some scale μ_0, which can be as low as 10^8 GeV, cf. Figs. 2 and 3. If that happens, our Universe becomes unstable[2].

---

[*] fedor.bezrukov@uconn.edu
[†] javier.rubio@epfl.ch
[‡] mikhail.shaposhnikov@epfl.ch
[1] The largest uncertainty comes from the determination of the top Yukawa coupling. Smaller uncertainties are associated to the determination of Higgs boson mass and the QCD gauge coupling α_s. See Refs. [3–5] for the most refined treatments and Ref. [6] for a review.
[2] The determination of the lifetime of the Universe is a rather subtle issue that strongly depends on the high energy completion of the SM. As shown in Ref. [7–9], if the gravitational corrections are such that the resulting effective potential lies above/below the SM one, the lifetime of our vacuum will be notably larger/smaller than the age of the Universe.
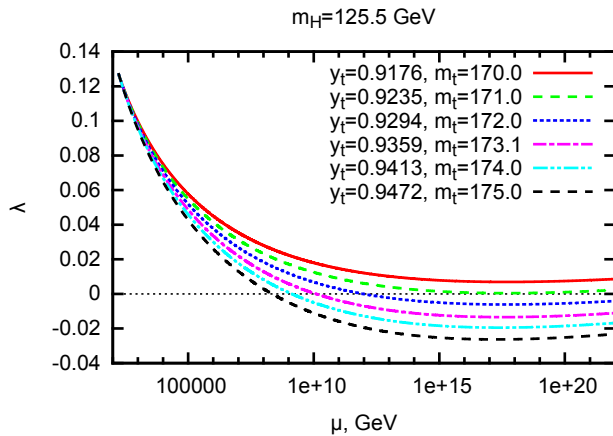

FIG. 1. Renormalization group running of the Higgs self-coupling for several values of the top quark Yukawa coupling (top pole mass) and fixed to 125.5 GeV Higgs boson mass.

The $0-3\sigma$ compatibility of the data with vacuum instability is one of the recurrent arguments for invoking new physics beyond the Standard Model. In particular, it is usually stated that the minimalistic Higgs inflation scenario [10], in which the Higgs field is non-minimally coupled to gravity with strength ξ, cannot take place if the Higgs self-coupling becomes negative at an energy scale below the inflationary scale.

We will show in this paper that Higgs inflation is possible *even if the SM vacuum is not absolutely stable*. Specifically, we will demonstrate that the renormalization effects at the scale M_P/ξ can bring the Higgs self-coupling λ to positive values in the inflationary domain. If that happens, inflation will take place with the usual chaotic initial conditions and the fate of the Universe will be inevitably determined by the subsequent evolution. At the end of the exponential expansion, the Higgs field will start to oscillate around the bottom of

the potential, which, contrary to the tree-level case, displays two minima, with the wider and deeper one located at very large Higgs values (cf. Fig. 4). The energy stored in the Higgs field right after the end of inflation *highly exceeds* the height of the barrier separating the minima. We will see that this leads to an interesting phenomenon. The oscillations of the Higgs field induce non-perturbative particle production, and eventually, reheat the Universe. The shape of the potential changes due to finite-temperature/medium effects. If the reheating temperature is sufficiently high, the symmetry gets restored and the extra minimum at large values of the Higgs field (temporally) disappears. The Higgs field rolls down the new potential and settles down in the electroweak vacuum. With the evolution of the Universe, the temperature decreases and the minimum at large field values reappears. However, since the probability of tunneling to the energetically more favorable state is completely negligible, the scalar field gets trapped near the true SM minimum and stays there till the present time.

The paper is organized as follows. In Section II we review the Higgs inflation model and the self-consistent approach to quantum corrections and higher-dimensional operators. The general arguments of Section II are quantified in Section III, where we discuss the contribution of the finite parts of counterterms to the effective potential and formulate the renormalization group equations for the coupling constants associated to them. In Section IV we explain how the renormalisation effects can allow for inflation to happen *even if our vacuum is metastable*. The temperature corrections to the effective potential are computed in Section V, where we determine the temperature T_+ at which the extra minimum at large field values disappears. Section VI is devoted to the study of reheating in non-critical and critical Higgs inflation and the estimation of the reheating temperature to be compared with T_+. Finally, the conclusions are presented in Section VII.

II. THE GENERAL FRAMEWORK

Higgs inflation is based on the observation that the Higgs-gravity Lagrangian

$$\mathcal{L} = \left(\frac{M_P^2}{2} + \xi H^\dagger H \right) R + g^{\mu\nu}(D_\mu H)^\dagger(D_\nu H) - \lambda(H^\dagger H)^2,$$
(2.1)

containing a non-minimal coupling of the Higgs field H to the Ricci scalar R can give rise to inflation for order one values of the Higgs self-coupling λ. When written in terms of a canonically normalized field in the Einstein frame, the model displays an asymptotically flat potential

$$V(\chi) = \frac{\lambda M_P^4}{4\xi^2} \left(1 - e^{-\sqrt{2/3}\kappa\chi} \right)^2,$$
(2.2)

which falls into the class of large field inflationary models. The value of the scalar field χ during inflation is of the
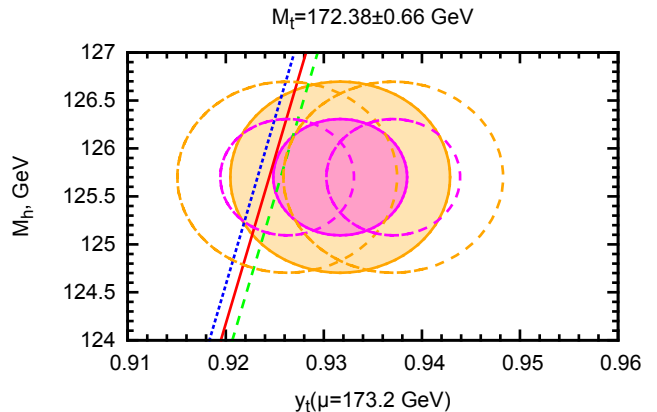

FIG. 2. (color online) The figure, taken from Ref. [6], shows the borderline between the regions of absolute stability and metastability of the SM vacuum on the plane of the Higgs boson mass and top quark Yukawa coupling in the $\overline{\text{MS}}$ scheme taken at $\mu = 173.2$ GeV. The diagonal line stands for the critical value of the top Yukawa coupling y_t^{crit} as a function of the Higgs mass and the dashed lines account for the uncertainty associated to the error in the strong coupling constant α_s. The SM vacuum is absolutely stable to the left of these lines and metastable to the right. The filled ellipses correspond to experimental values of y_t extracted from the latest CMS determination [11] of the Monte-Carlo top quark mass $M_t = 172.38 \pm 0.10\,(\text{stat}) \pm 0.65\,(\text{syst})$ GeV, if this is identified with the pole mass. Dashed ellipses encode the shifts associated to the ambiguous relation between pole and Monte Carlo masses. The ellipses are displaced to the right if other determinations of the Monte-Carlo top mass are used, $M_t = 173.34 \pm 0.27\,(\text{stat}) \pm 0.71\,(\text{syst})$ GeV and $M_t = 174.34 \pm 0.37\,(\text{stat}) \pm 0.52\,(\text{syst})$ GeV coming respectively from the combined analysis of ATLAS, CMS, CDF, and D0 data (at 8.7 fb^{-1} of Tevatron Run II) [12] and from the CDF and D0 combined analysis of Run I and Run II of Tevatron [13].
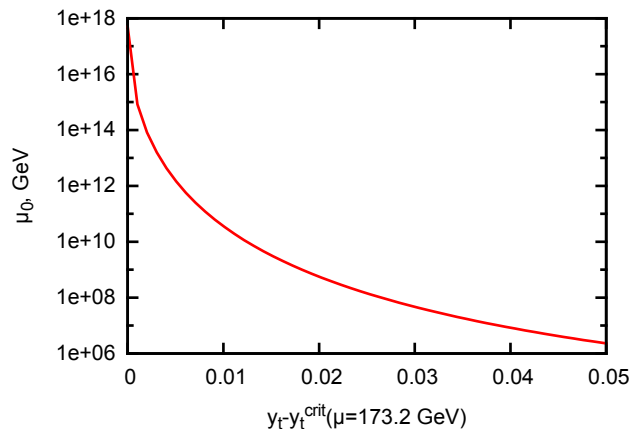

FIG. 3. Energy scale μ_0 where the Higgs self-coupling becomes negative as a function of the deviation of the top Yukawa coupling y_t from the critical value y_t^{crit}. Adapted from Ref. [6].
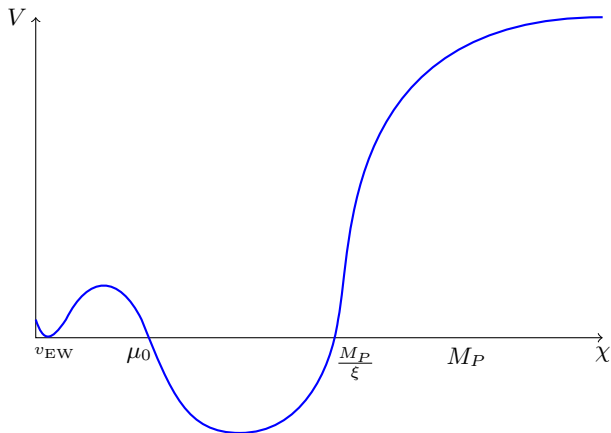
FIG. 4. Sketch of the effective Higgs inflation potential for the scenario considered in this paper. It contains an inflationary plateau at $\chi \gtrsim M_P$ and two minima. The shallowest and narrowest one is the standard electroweak vacuum v_{EW}. The deepest and widest one is generated by the interplay between the instability of the Higgs self-coupling beyond the scale μ_0 and the renormalization effects appearing at the scale M_P/ξ.

order of the reduced Planck mass $M_P = \kappa^{-1} = 2.435 \times 10^{18}$ GeV and it is related to the Higgs field in the unitary gauge ($H = (0, h/\sqrt{2})^T$) in a well defined manner

$$\frac{d\chi}{dh} = \sqrt{\frac{\Omega^2 + 6\xi^2 h^2/M_P^2}{\Omega^4}}, \quad (2.3)$$

where

$$\Omega^2 = 1 + \xi h^2/M_P^2 , \quad (2.4)$$

stands for the conformal factor giving rise to the Einstein frame. At the classical level, the model predicts a Gaussian spectrum of primordial fluctuations with a universal spectral index for scalar perturbations ($n_s \simeq 0.97$) and a small tensor-to-scalar ratio ($r \simeq 0.003$) [10]. The normalization of scalar perturbations at large scales fixes the ratio λ/ξ^2 in Eq. (2.2). No relation between particle physics and cosmological parameters shows up. The variation of the self-coupling λ, associated with a change of the Higgs boson mass, can be always compensated by the change of the (a-priori unknown) non-minimal coupling ξ. For $\lambda \sim \mathcal{O}(1)$, ξ is required to be rather large, $\xi \sim \mathcal{O}(10^4)$, but still significantly smaller than the value giving rise to noticeable effects in low energy experiments [10].

The link between the SM parameters and cosmological observations appears when quantum effects are taken into account. The inclusion of quantum corrections is a non-trivial task. When written in the Einstein frame, the Lagrangian (2.1) is essentially non-polynomial and therefore non-renormalizable. This immediately poses a number of questions:

A. "What is the sensitivity of Higgs inflation to the higher dimensional operators that should be included into the analysis? Which is the proper ultraviolet cutoff?"

B. "Can we do reliable computations of radiative corrections in a non-renormalizable theory?"

C. "What is the running of the SM couplings to the inflationary scale where the Higgs inflation potential should be computed? What is the relation between low and high energy parameters?"

In the absence of an ultraviolet completion for the SM non-minimally coupled gravity, the answer to these questions can be only based on the *self-consistency* of the procedure. This was indeed the attitude taken in Ref. [14], where the effective field theory for Higgs inflation was formulated (some further developments can be also found in Ref. [15]). In what follows we summarize the main assumptions and results of this approach and provide answers to the questions A, B and C.

A. Sensitivity to higher dimensional operators

Let us denote by Λ the suppression scale of the higher dimensional operators to be added to the SM.[3] The value of Λ is a-priori unknown and depends on the different thresholds (masses of new particles) that were integrated out to get the low-energy effective field theory. In principle, it could be as large as the Planck mass M_P, where gravitational interactions become important for sure. In that case, the effect of higher-dimensional operators such as h^6/M_P^2 would be numerically small for sufficiently large ξ.[4]

Although quite natural, the identification of the cutoff scale with the Planck mass may turn out to be theoretically inconsistent since other processes can break tree-level unitarity at lower energies [14, 16–18]. A self-consistent approach is to define the parameter Λ from the theory itself by considering all the possible reactions between the SM constituents.

The energy scale signaling the breaking of tree-level unitarity in particle collisions depends on the expectation value of the background field h. At small field values ($h \lesssim M_P/\xi$), the cutoffs associated to the different interactions agree with the result of the naive computation performed around the electroweak vacuum, $\Lambda(h) \simeq M_P/\xi$. At large field values ($h \gtrsim M_P/\sqrt{\xi}$), the suppression scale depends on the particular scattering process considered. The suppression of graviton-graviton interactions is particularly strong and coincides with the dynamical Planck scale $\Lambda^2(h) \simeq \xi_h h^2$. The lowest cutoff

---

[3] For concreteness, the discussion in this section is based on the Jordan frame Lagrangian (2.1).
[4] For typical inflationary field values $h \propto M_P/\sqrt{\xi}$, the correction to inflationary energy density is of order $\delta V_{\text{infl}}/V_{\text{infl}} \sim 1/(\xi\lambda)$.

dictated by the theory appears in the gauge sector and grows linearly with the field, $\Lambda(h) \sim h$

All the relevant scales involved in the inflationary and post-inflationary evolution of the Universe (i.e. the Hubble rate and the reheating temperature of the Universe) are parametrically smaller than the previous cutoffs. As a consequence of this, the weak coupling approximation remains valid and the cosmological predictions of the Higgs inflation are stable against the addition of higher-dimensional operators introduced along the lines of the standard effective field theory reasoning [14] (see also Ref. [19]).

B. Reliability of the computation of radiative corrections

Since the SM (itself renormalizable) is coupled to gravity, the resulting theory is clearly non-renormalizable. According to the general rules of quantum field theory, a sensible computation of radiative corrections requires the addition of an infinite number of counterterms together with the choice of a subtraction scheme.

The structure of the counterterms will be similar to that of the higher dimensional operators discussed above, but with their precise form fixed by the requirement of removing the divergencies in the loop diagrams steaming from the initial Lagrangian.

A subtraction scheme that fits well with the assumption of not having new heavy particles between the electroweak and the Planck scale is dimensional regularization, since it effectively ignores power-like divergences. The standard procedure in this prescription is to compute the one loop effective action from the tree-level Lagrangian density (2.1), expand it in Laurent series in $\epsilon = (4 - D)/2$ (with D the fractional dimension of space-time), and add to it the necessary operators O_n with coefficients $A_n/\epsilon + B_n$ to remove the divergences. The process can be extended recursively to higher order loops. While the coefficients A_n are fixed by the structure of divergences, the coefficients B_n are arbitrary. This creates the first source of uncertainties [14].

A second source of uncertainties is associated with the choice of the normalization point μ, which, in dimensional regularization, corrects the mismatch in the mass dimension of the coupling constants. In renormalizable field theories, μ is arbitrary and space-time independent. Although we could certainly maintain this prescription for our non-renormalizable field theory[5], nothing prevents us from modifying it and allow μ to be field dependent. Among the many different possibilities, we will consider the combination[6]

$$\mu^2 \propto M_P^2/2 + \xi H^\dagger H . \qquad (2.5)$$

The reason for this choice is twofold. On the one hand, it allows to maintain the quantum version of the theory asymptotically scale-invariant at large values of the Higgs field ($h \gg M_P/\sqrt{\xi}$). On the other hand, it becomes the standard (space-time independent) prescription of renormalizable field theories when written in the Einstein frame.

It may seem that an arbitrariness of the coefficients B_n results on the loss of predictivity of the Higgs inflation. However, as it was shown in Ref. [14], the finite parts of the counterterm do not change the asymptotic behavior of the scalar potential. The predictions of Higgs inflation fall into two categories:

1. *Universal/Non-critical regime*: For a large fraction of the parameter space, the renormalization group enhanced (RGE) potential maintains the shape and predictions of the tree-level potential. As (2.2), the RGE potential depends on λ and ξ only through the combination λ/ξ^2. Taking into account the COBE normalization and the value of the Higgs self-coupling at the inflationary scale, we can univocally fix the value of ξ, which turns out to be of order $\xi \sim \mathcal{O}(10^3)$. Although the non-minimal coupling is still rather large, the difference between the scale below which the SM is valid without modifications ($M_P/\xi \sim 3 \times 10^{15}$ GeV) and the scale at which inflation takes place ($M_P/\sqrt{\xi} \sim 10^{17}$ GeV) is relatively small.

2. *Critical regime*: For very specific values of the SM parameters, the second derivative of the RGE potential become equal to zero at some intermediate field value between the beginning and the end of inflation. The first derivative is extremely small in the same point (but nonvanishing). This gives rise to a non-monotonic behavior of the slow-roll parameter ϵ and opens the possibility of obtaining a sizable tensor-to-scalar ratio r, whose precise value strongly depends on ξ and on the Higgs and top Yukawa couplings at the inflationary scale [15, 25]. The non-minimal coupling ξ is generically rather small ($\xi \sim 10$) and the model does not require the inclusion of a cutoff scale significantly below the Planck scale (cf. Section II A).

C. Relation between low and high energy parameters

An analysis of Higgs inflation and its connection with low energy observables has been presented in Refs [14,

---

[5] This would correspond to the the Jordan frame prescription II of Ref. [20], used in Refs. [21–24]

[6] This is the Jordan frame prescription I in Ref. [20]. The analysis with other μ choices is left for future investigations.

15]. The self-consistent set of assumptions about non-renormalizable contributions to the action of the theory is formulated as follows:

i. We will only add the higher dimensional operators that are generated via radiative corrections by the Lagrangian of the SM non-minimally coupled to gravity. In other words, only a subclass of the operators described in Section II B will be considered.

ii. The coefficients B_n are small ($B_n \ll 1$) and have the same hierarchy as the loop corrections producing them, i.e. the coefficients in front of the operators coming from two-loop diagrams are much smaller than those coming from one-loop diagrams, etc.

iii. The renormalization scale is chosen as in (2.5). This is equivalent to the requirement of scale invariance of the UV complete theory at large values of the Higgs field background.

None of these assumptions is essential for the scenario presented in this paper, but they are needed to provide a (partially) controllable link between the low energy and high energy parameters of the model.

In this framework, the relation between *low energy parameters*, such as the Higgs mass or the top quark Yukawa coupling y_t, and the high energy parameters fixing the form of the effective potential in the inflationary region does depend on the unknown coefficients B_n, which should be fixed by an eventual ultraviolet completion.

For $h \lesssim M_P/\xi$ the contribution of the higher order operators O_n defined in Section II B is suppressed. The theory is effectively renormalizable and the running of the coupling constants is governed by the usual SM renormalization group (RG) equations. In the inflationary region, i.e for $h \gtrsim M_P/\sqrt{\xi}$, the radial component of the Higgs field is effectively frozen and the evolution of the coupling constants is determined by the renormalization group equations of the chiral Standard Model [26] . In both regimes, the coefficients B_n do not play any role, because of the specific asymptotics of the operators O_n as functions of the Higgs field. However, in the transition region around $h \simeq M_P/\xi$, the coupling constants change rapidly (very roughly, making a jump) by an amount proportional to the coefficients B_n in front of the corresponding operators O_n.

In the following section, we will compute the effective potential and will determine the magnitudes and signs of the coefficients B_n giving rise to Higgs inflation in the case of a metastable electroweak vacuum.

III. HIGH ENERGY VERSUS LOW ENERGY PARAMETERS OF THE STANDARD MODEL

In this section we settle the formalism to obtain the effective action in the whole region between the SM-like regime ($\phi \ll M_P/\xi$) and the inflationary regime ($\phi > M_P/\sqrt{\xi}$). The approach described in this section closely follows the one outlined in Section 3 of Ref. [14]. Throughout this section we work exclusively in the Einstein frame and neglect the higher order corrections in slow roll, i.e. we assume that all the important effects are described by the corrections to the effective potential.

Following the discussion of Section II B, we will compute the effective action in dimensional regularization, where all power-like divergences are systematically ignored. We will concentrate on the most important contribution: the one associated to the Higgs and top quark interactions[7]. The relevant piece of the Einstein frame Lagrangian density is given by[8]

$$\mathcal{L} = \frac{(\partial\chi)^2}{2} - \frac{\lambda}{4}F^4(\chi) + i\bar{\psi}_t \slashed{\partial}\psi_t + \frac{y_t}{\sqrt{2}}F(\chi)\bar{\psi}_t\psi_t \,. \quad (3.1)$$

The function $F(\chi) \equiv h(\chi)/\Omega(\chi)$ coincides with the Higgs field at low energies and encodes all the non-linearities associated to the non-minimal coupling to gravity in the large field regime

$$F(\chi) \approx \left\{ \begin{array}{l} \chi \qquad\qquad\qquad\qquad\quad , \chi < \frac{M_P}{\xi} \\ \frac{M_P}{\sqrt{\xi}}\left(1 - e^{-\sqrt{2/3}\kappa\chi}\right)^{1/2} , \chi > \frac{M_P}{\xi} \end{array} \right\} , \quad (3.2)$$

with $\kappa = M_P^{-1}$.

A. Higgs coupling

Let us start by computing the effective potential for (3.1) at one loop. We get the following two vacuum diagrams

$$\includegraphics = \frac{1}{2}\,\mathrm{Tr}\ln\left[\Box - \left(\frac{\lambda}{4}(F^4)''\right)^2\right] \,, \quad (3.3)$$

$$\includegraphics = -\,\mathrm{Tr}\ln\left[i\slashed{\partial} + y_t F\right] \,, \quad (3.4)$$

whose evaluation, using the standard techniques, gives

$$\includegraphics = \frac{9\lambda^2}{64\pi^2}\left(\frac{2}{\bar{\epsilon}} - \ln\frac{\lambda(F^4)''}{4\mu^2} + \frac{3}{2}\right)\left(F'^2 + \frac{1}{3}F''F\right)^2 F^4,$$

$$\includegraphics = -\frac{y_t^4}{64\pi^2}\left(\frac{2}{\bar{\epsilon}} - \ln\frac{y_t^2 F^2}{2\mu^2} + \frac{3}{2}\right)F^4 \,. \quad (3.5)$$

Here $2/\bar{\epsilon}$ stands for the combination $2/\epsilon - \gamma + \ln 4\pi$ and the primes denote derivatives with respect to χ. The divergencies in the loop diagrams (3.5) are eliminated, as

---

[7] All other SM particles may be added and treated analogously.

[8] For illustrative purposes we will neglect the $SU(2)$ structure of the Higgs doublet and the colors of the top quark. These are not important for the derivation of Eqs. (3.7) and (3.11).

usual, by adding counterterms with the definite coefficients in $1/\bar{\epsilon}$ and arbitrary finite parts $\delta\lambda_1$ and $\delta\lambda_2$

$$\delta\mathcal{L}_{\text{ct}} = \left(-\frac{2}{\epsilon}\frac{9\lambda^2}{64\pi^2} + \delta\lambda_1\right)\left(F'^2 + \frac{1}{3}F''F^2\right)^2 F^4$$
$$+ \left(\frac{2}{\epsilon}\frac{y_t^4}{64\pi^2} - \delta\lambda_2\right)F^4. \qquad (3.6)$$

The effective potential is the sum of (3.1), (3.5), and (3.6), with the poles in $1/\bar{\epsilon}$ canceling between the counterterms and the 1-loop contributions. The structure of the counterterm involving $\delta\lambda_2$ coincides with that of the tree-level potential (2.2). This allows us to eliminate the constant $\delta\lambda_2$ by incorporating it into the definition of λ. The constant $\delta\lambda_1$, on the contrary, cannot be reabsorbed[9].

The value of λ at the inflationary scale ($\chi \sim M_P$) depends on the counterterm (3.6). For small field values ($F(\chi) \sim \chi \ll M_P/\xi$), the conformal factor $\Omega(\chi)$ equals to one and the theory becomes indistinguishable from the renormalizable SM. In that case, the first term in Eq. (3.6) turns into a simple $\delta\lambda_1\chi^4/4$ term, which allows to reabsorb the constant $\delta\lambda_1$ into the definition of λ. At large field values ($F(\chi) \sim M_P/\sqrt{\xi}$, $\chi \gtrsim M_P$), the counterterm is exponentially suppressed ($\sim \delta\lambda\frac{M_P^4}{\xi^4}e^{-4\chi/\sqrt{6}M_P}$) and the previously absorbed contribution to λ effectively disappears. Neglecting the running of $\delta\lambda_1$ between the scales $\mu \sim M_P/\xi$ and $M_P/\sqrt{\xi}$, we can imitate this effect by a change

$$\lambda(\mu) \to \lambda(\mu) + \delta\lambda\left[\left(F'^2 + \frac{1}{3}F''F\right)^2 - 1\right], \qquad (3.7)$$

where $\lambda(\mu)$ is evaluated using the SM RG equations. Since the effective potential is μ-independent, we can choose the most convenient value of μ. In order to minimize the logarithms in the 1-loop contributions[10], we will take
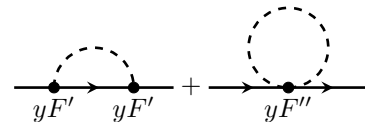
$$\mu^2 = \alpha m_t(\chi) = \alpha y_t F(\chi), \qquad (3.8)$$

with α a constant of order one.

B. Top Yukawa coupling

The effect described above applies also to the Yukawa coupling. To see this, consider the propagation of the top

———

[9] Indeed it should be promoted to a new independent coupling constant with its own RG equation. The RG equations are obtained by requiring the Lagrangian density $\mathcal{L} + \delta\mathcal{L}$ to be independent of μ. Since we are dealing with a non-renormalizable theory, the set of RG equations is not closed. We postpone the derivation of these equations to a future publication and will assume that the (infinite) system of equations can be truncated due to the point (ii) in Section II C.

[10] If the logarithms were large one should add higher loop contributions.

quark in the background χ

$$(3.9)$$

Cancelling divergencies in these diagrams requires the counterterms of the form

$$\delta\mathcal{L}_{\text{ct}} \sim \left(\#\frac{y_t^3}{\bar{\epsilon}} + \delta y_{t1}\right)F'^2 F\bar{\psi}\psi$$
$$+ \left(\#\frac{y_t\lambda}{\bar{\epsilon}} + \delta y_{t2}\right)F''(F^4)''\bar{\psi}\psi, \qquad (3.10)$$

where $y_t F'$ appears from the vertices with one Higgs field, $y_t F''$ from vertices with two Higgs fields, $y_t F$ from the mass of the top-quark in the propagator and $\lambda(F^4)''$ from the mass of the scalar propagator in the bubble. The term with δy_{t1} has similar properties to that with $\delta\lambda_1$. In the limit of small χ it goes as $\chi\bar{\psi}\psi$, and it can be reabsorbed into the definition of the Yukawa coupling y_t (as in the SM). For large χ, the counterterm vanishes and the contribution δy_t into y_t disappears. As before, we neglect the running of δy_{t1} between M_P/ξ and $M_P/\sqrt{\xi}$ and parametrize this effect by an effective change

$$y_t(\mu) \to y_t(\mu) + \delta y_t\left[F'^2 - 1\right], \qquad (3.11)$$

with μ given by Eq. (3.8).

IV. HIGGS INFLATION WITH METASTABLE VACUUM

If the "jumps" $\delta\lambda$ and δy_t are much smaller than the respective coupling constants at the transition scale M_P/ξ ($\delta\lambda \ll \lambda(M_P/\xi)$, $\delta y_t \ll y_t(M_P/\xi)$), Higgs inflation requires the absolute stability of the vacuum and provides a clear connection between the properties of the Universe at large scales and the value of the SM Higgs and top quark masses. However, since the smallness of λ at the inflationary scale appears as the result of a non-trivial cancellation between the fermionic and bosonic contributions, it is considerable to think that $\delta\lambda$ can be of order λ. In that case, the "jumps" of the coupling constants open the possibility of having Higgs inflation even in the case of a metastable vacuum by converting a negative scalar self-coupling below M_P/ξ into a positive coupling above that scale. Some illustrative values of the tparameters needed to restore non-critical Higgs inflation beyond an instability scale μ_0 are presented in Table I.

The effect of the coefficients $\delta\lambda$ and δy_t on the running of the coupling λ and y_t is summarized in Fig. 5. Qualitatively, the coefficient $\delta\lambda$ controls the height of the potential in the inflationary region, while the coefficient δy_t controls the tilt. As schematically represented in Fig. 4, the associated (zero temperature) effective potential has an inflationary plateau at large values of the scalar field,

$m_h = 125.5$ GeV	$\xi = 1500$	$\delta y_t \simeq 0.025$
m_t	μ_0 (GeV)	$\delta\lambda$
172.0	$\sim 2 \times 10^{12}$	-0.008
173.1	$\sim 2 \times 10^{10}$	-0.015
174.0	$\sim 2 \times 10^{9}$	-0.022
175.0	$\sim 3 \times 10^{8}$	-0.029

TABLE I. Illustrative values of the top pole mass m_t and the associated instability scale μ_0 for fixed values of the Higgs mass m_h and the non-minimal coupling to gravity ξ. The values of $\delta\lambda$ are chosen to restore the asymptotic behavior of the potential at the inflationary scale. All choices of parameters give roughly the same inflationary predictions.
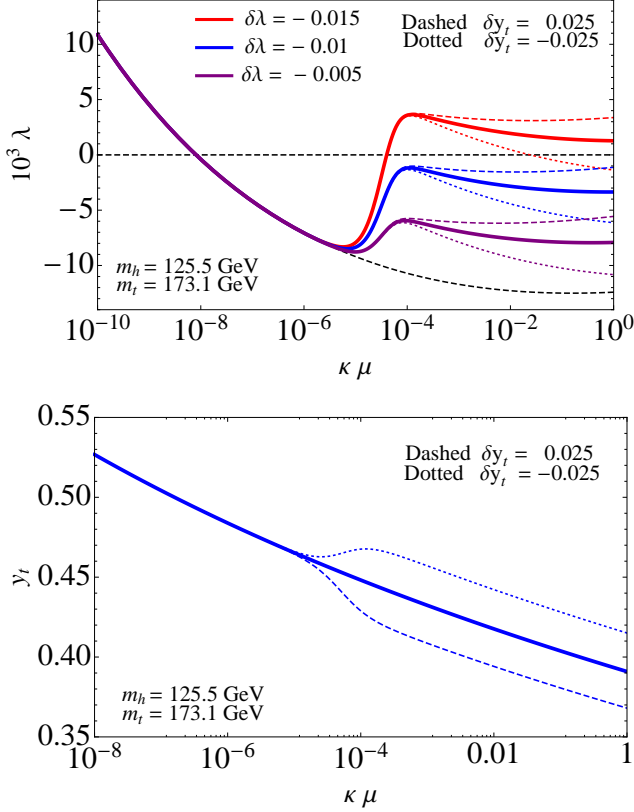
FIG. 5. (color online) Effect of the coefficients $\delta\lambda$ and δy_t on the running of λ and y_t as a function of the field-dependent renormalization scale $\mu(\chi)$ in Planck units ($\kappa = M_P^{-1}$).

and two minima. The first one (the shallowest and narrowest one) corresponds to the standard electroweak vacuum. The second one (the deepest and widest one) is generated by the interplay between the instability of the Higgs self-coupling below M_P/ξ and the jumps at that scale. As in any chaotic inflation scenario, the Higgs field will start its evolution from trans-Planckian values, will inflate the Universe and will decay into the SM particles after the exponential expansion [27]. At first sight, it may seem that, at the end of this set of processes, the universe
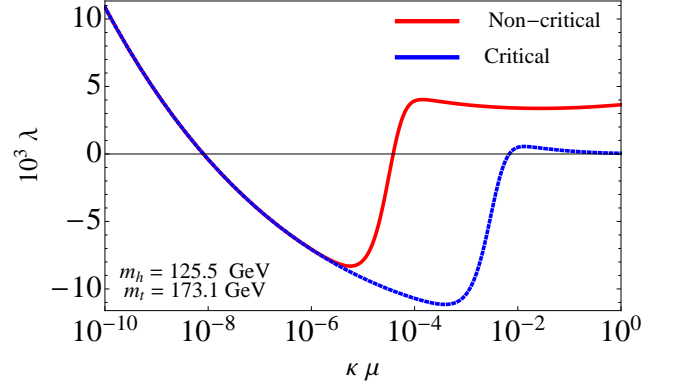

FIG. 6. (color online) Comparison between the running of the Higgs self-coupling λ in the critical ($\xi = 15$, $\delta y_t = 0$, $\delta\lambda = -0.0133$) and non-critical ($\xi = 1500$, $\delta y_t = 0.025$, $\delta\lambda = -0.015$) cases as a function of the field-dependent renormalization scale $\mu(\chi)$ in Planck units ($\kappa = M_P^{-1}$).

will end at the deeper and wider vacuum at $\chi \sim M_P/\xi$. However, this is not necessarily the case. The destiny of the Universe strongly depends on the relation between the energy stored in the Higgs field after inflation and the depth of the minimum at large fields values. If the first one is much larger than the second, the reheating of the Universe after inflation may result into a sizable modification of the effective potential, leading to the disappearance of the "dangerous" vacuum at large field values and the subsequent evolution of the system towards the "safe" electroweak vacuum. On the contrary, if the two energy scales are comparable, the Universe will end in the "dangerous" vacuum and will inevitably collapse [28].

The depth and width of the extra minimum is effectively controlled by the non-minimal coupling ξ, which determines the value $\chi \sim M_P/\xi$ at which the transition from negative to positive λ takes place (cf. Fig. 6)[11]. At the same time, ξ is the main parameter distinguishing the non-critical and critical scenarios[12]. The dual role of ξ allows to conclude that the depth of the minimum is generically much smaller than the scale of inflation in the non-critical case and comparable to it in the critical one. Critical Higgs inflation is then expected to require the absolute stability of the vacuum.

The following sections are devoted to quantify the general arguments presented above. In Section V, we will discuss the finite temperature effective potential and de-

---

[11] Strictly speaking, the values of the parameters for the non-critical case presented in Fig. 6 *do not* give give to realistic values of the inflationary observables and are included just for illustration purposes. The proper analysis of the parameter space in critical Higgs inflation is extremely subtle and we postpone it to a future work.

[12] Note that these two regimes can be distinguished cosmologically, as far as in the non-critical case the tensor to scalar ratio is small, while in the critical case it can be rather large.

termine the minimal temperature T_+ needed to restore the stability of the potential in the non-critical and critical cases. By comparing this temperature with the upper bounds on the reheating temperature T_{RH} obtained in Section VI, we will demonstrate that $T_{RH} > T_+$ in non-critical case and that $T_{RH} < T_+$ in the critical one.

V. HIGH TEMPERATURE EFFECTIVE POTENTIAL

The set of coefficients presented in Table I makes the Higgs self-coupling positive at large values of the Higgs field and allows for inflation. However, the zero-temperature effective potential has an extra minimum at large values of the scalar fields. In this section, we consider the change in the shape of the effective potential in the presence of a thermal plasma, as that originated by the decay of the inflaton into the SM particles. In particular, we will determine the minimum temperature needed to stabilize the effective potential and the temperature needed to drive the Higgs field towards the true electroweak minimum.

The one-loop finite temperature corrections can be written in the form [29]

$$\Delta V_T = -\frac{1}{6\pi^2} \sum_{B,F} \int_0^\infty \frac{k^4 dk}{\epsilon_k(m_{B,F})} n_{B,F}[\epsilon_k(m_{B,F})] \, . \quad (5.1)$$

Here n_B and n_F are the Bose and Fermi distributions $n_{B,F}[x] = 1/(e^{x/T} \mp 1)$, $\epsilon_k(m) = \sqrt{k^2 + m^2}$, $m_{B,F}$ are the masses of SM particles in the background Higgs field, and the summation is over all the SM degrees of freedom. The most important contributions come from the top quark and the gauge bosons, with masses

$$m_Z^2(T) = \frac{g_1^2(\mu_g) + g_2^2(\mu_g)}{4} F^2(\chi), \quad (5.2)$$

$$m_W^2(T) = \frac{g_2^2(\mu_g)}{4} F^2(\chi), \quad (5.3)$$

$$m_t(T) = \frac{y_t(\mu_t)}{\sqrt{2}} F(\chi). \quad (5.4)$$

The coupling constants in the previous expressions should be taken at the relevant scale, which can be always chosen proportional to the temperature.[13] The thermally

----

[13] The coupling constants appearing in boson loops were evaluated at the scale $\mu_g = 7T$. On the other hand, those appearing in fermion loops were evaluated at the scale $\mu_t = 1.8T$. As shown in Ref. [30], this choice minimizes radiative corrections. The previous two choices should be replaced by more complicated expressions involving χ and T in the limit of low temperatures (smaller that the background field scale). This change is however irrelevant from a numerical point of view, since in that case the thermal potential (5.1) is exponentially suppressed.
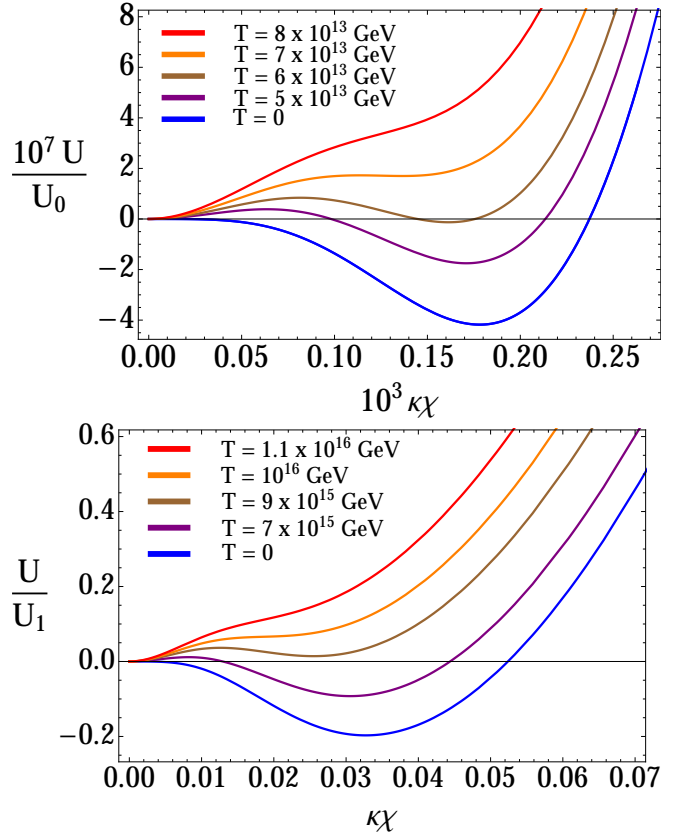

FIG. 7. Top: High temperature effective potential for non-critical Higgs inflation ($m_H = 125.5\,\text{GeV}$, $m_T = 173.1\,\text{GeV}$, $\xi = 1500$, $\delta y_t = 0.025$, $\delta\lambda = -0.0153$). Bottom: High temperature effective potential for critical Higgs inflation ($m_H = 125.5\,\text{GeV}$, $m_T = 173.1\,\text{GeV}$, $\xi = 15$, $\delta y_t = 0$, $\delta\lambda = -0.01325$).

corrected effective potential for the non-critical/critical case is shown in the upper/lower part of Fig. 7. In the noncritical case, the restoration temperature and the temperature at which the minimum at high field values of the Higgs field disappears are given respectively by

$$T_-^{NC} \simeq 6 \times 10^{13} \text{ GeV}, \qquad T_+^{NC} \simeq 7 \times 10^{13} \text{ GeV}. \quad (5.5)$$

The associated temperatures in the critical case turn out to be significantly larger[14]

$$T_-^C \simeq 9 \times 10^{15} \text{ GeV}, \qquad T_+^C \simeq 10^{16} \text{ GeV}. \quad (5.6)$$

If the Universe is heated up to the temperatures T_{RH} above T_+, the system will relax to the SM vacuum. In the subsequent evolution of the Universe the temperature decreases and the second minimum reappears at large field values, first as a local minimum, then as the global

----

[14] Remember that the second minimum of the potential is much wider and deeper in the critical case.
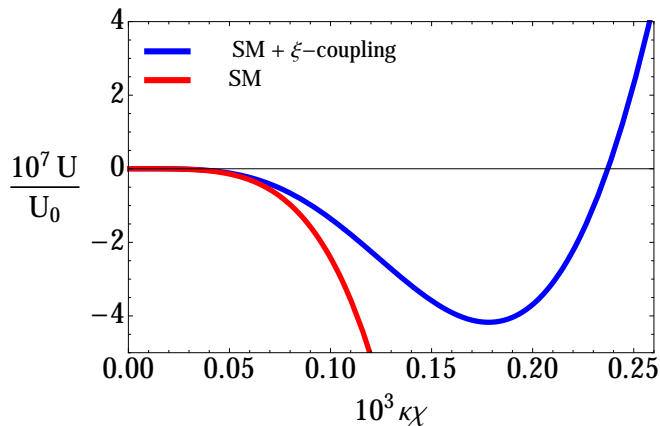
FIG. 8. Comparison between the effective potential for the SM and the SM non-minimally coupled to gravity ($\xi = 1500$, $\delta y_t = 0$, $\delta\lambda = -0.017$). The normalization scale $U_0 = (10^{-3}M_P)^4$ coincides with that in Fig. 9 and $\kappa = M_P^{-1}$. Since the potential for the non-minimally coupled case lays on top of the SM, the lifetime of the Universe in Higgs inflation is even larger than in the SM alone.

one. However, there is always a barrier separating these two minima (not really visible on the plot due to the overall χ^4 behavior at low field values). This barrier prevents the direct decay of the Fermi vacuum. The decay of the SM vacuum can still happen via tunneling, but the probability of this process turns out to be rather small. The probability of the decay of the EW vacuum due to thermal fluctuations in the absence of gravity was studied in Refs. [31–34], with the result that this effect does not lead to the vacuum decay for the present day values of the Higgs and top quark masses. Since the thermal potential is always above the SM one (cf. Fig. 8), the probability of decay in our case is even smaller than in the absence of gravity and can be safely neglected.

The aim of the next sections is to estimate the reheating temperature T_{RH} in the critical and non-critical cases. It should be noted that the effect of the symmetry restoration discussed above *does not require thermal equilibrium* [35]. What is important is that the medium effects change the effective potential in such a way that the positive contributions to the scalar mass are generated. The effective temperature T_* that can be used for an estimate of the medium effects can be defined through the typical integrals that appear in the computation of the effective potential,

$$\frac{T_*^2}{24} \simeq \int \frac{d^3k}{2|k|(2\pi)^3} n_{B,F}^{\text{noneq}} , \qquad (5.7)$$

where $n_{B,F}^{\text{noneq}}$ are the distributions of the particles created at preheating. The preheating temperate T_{RH} determined in the next sections is generically smaller than T_* and it should be then understood as a *conservative* estimate of the temperature to be compared with the restoration temperature T_+.

VI. PREHEATING

Determining the proper reheating temperature is a rather complicated task. It generically requires the use of numerical simulations able to deal with the highly non-linear and non-perturbative particle production after inflation together with a detailed analysis of the thermalization stage (see Refs. [36, 37] for a review). In this section, we will simply try to provide a rough estimate of this temperature based on the following considerations:

1. At the end of inflation the Higgs field oscillates around the minimum of the potential. During each semioscillation j, the SM fields coupled to it oscillate many times and particle creation takes place. The depletion of the Higgs condensate is dominated by the production of W and Z bosons[15,16] and their subsequent decay into relativistic SM fermions.

   The interplay between non-perturbative particle creation and decays will be accounted for using the *combined preheating* formalism [38, 39], which allows to estimate the energy density of the different species as a function of the number of semioscillations (cf. Appendix C for details and notation). The beginning of the radiation domination era will be determined by the time at which the energy in the relativistic fermions equals the energy density in the homogeneous background field.

2. At the time of production, the distribution of fermions is far from thermal. To achieve equilibrium, they must interact to redistribute their energy (kinetic equilibrium) and to adjust their number density (chemical equilibrium). As shown in Ref. [40] (see also Refs. [41–43]), the particular way in which this happens depends on the relative occupancy of the produced plasma with respect to a thermal distribution. To determine if we are dealing with an under- or an over-occupied system, we will define an instantaneous "radiation temperature"[17]

$$T_r(j) \equiv \left(\frac{30\rho_F(j)}{g_*\pi^2}\right)^{1/4} , \qquad (6.1)$$

and we will compare the number density and average energy per particle in our plasma to those of a

_____

[15] The direct production of fermions is suppressed by Pauli blocking effects.
[16] The creation of Higgses, although tachyonic in nature, is much less efficient (cf. Appendix B for details).
[17] This temperature is obtained by equating the total energy density of the fermions at a given time, $\rho_F(j)$, to the energy density of a thermal plasma in thermal equilibrium.
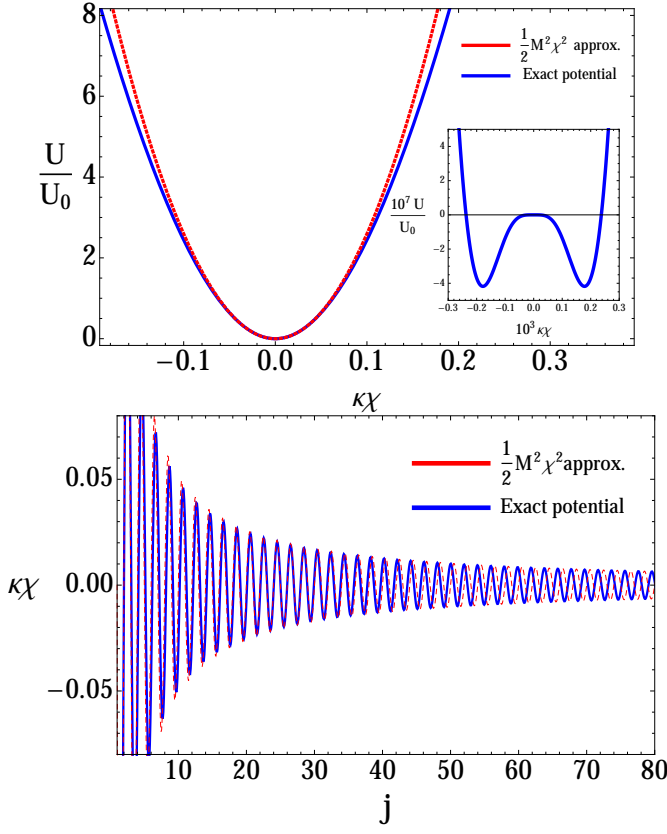
FIG. 9. (color online) Top: Comparison between the exact renormalization group enhanced potential in the non-critical case and the quadratic approximation (A1). The normalization scale U_0 is taken to be $U_0 = (10^{-3}M_P)^4$ and $\kappa = M_P^{-1}$.. Bottom: Evolution of the background field χ in the non-critical case as a function of the number of oscillations j. Field values are measured in Planck units ($\kappa = M_P^{-1}$).

thermal gas containing the same number degrees of freedom[18], namely

$$n_{\text{th}}(j) = \frac{3\zeta(3)}{4\pi^2} g_* T_r(j)^3 \,, \qquad (6.2)$$

$$\langle E_{\text{th}}(j)\rangle = \frac{7\pi^4}{180\zeta(3)} T_r(j) \,. \qquad (6.3)$$

A. Non-critical Higgs inflation

As shown in Fig. 9, the RGE potential for non-critical Higgs inflation can be well approximated by a quadratic potential, except for the very small fields values $\chi \sim$

---

[18] The factor g_* stands the number of degrees of freedom resulting from the decay of W and Z bosons. Since the top quark is not produced in these decays, we will take $g_* = (4 \times 3 + 2 \times 3 + 4 \times 3 \times 5) = 68.25$.
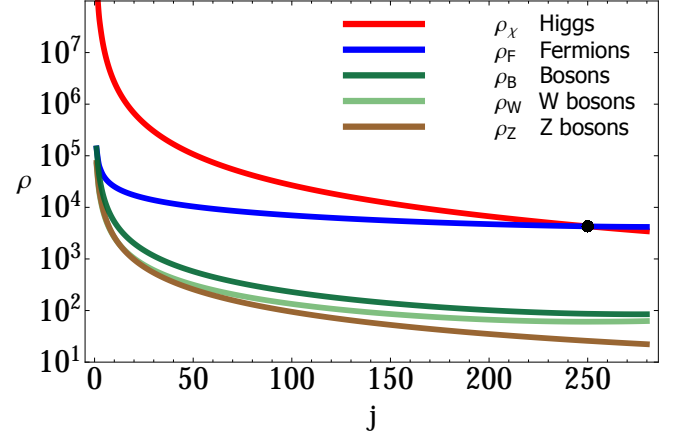

FIG. 10. (color online) Evolution of the different energy densities (in M^4 units) for the non-critical case ($\lambda = 3.4 \times 10^{-3}$, $\xi = 1500$, $g_1 = 0.44$, $g_2 = 0.53$) as a function of the number of semioscillations j.

$\mathcal{O}(10^{-4})M_P$ in which the self-coupling of the Higgs field becomes negative. For a large number of oscillations, the evolution of the Higgs field is completely unaffected by the features of the potential at small field values. This allows to apply the combined preheating formalism presented in Appendix B.

The energy densities for the created gauge bosons and fermions[19] (cf. Eqs. (A16), (A17), (A18) and (A25)) as a function of the number of semioscillations j are presented in Fig. 10. The production of W and Z particles in the first semioscillation is significantly larger than in the tree-level case[20]. The continuous production and subsequent decay rapidly sustains the energy density of the fermions against the expansion of the Universe. Radiation domination takes place after $j_r = 250$ semioscillations and precedes the onset of parametric resonance. The backreaction of the gauge bosons and fermions *on the effective oscillation frequency* can be completely neglected at that time (cf. Appendix C).

As shown in Fig. 11, soon after the beginning of preheating, the sustained evolution of the total number of fermions due to particle creation together with the redshift of energies $E_{F(B)}$ due to the expansion of the Universe drives the system into an overoccupied state made of low energetic particles with respect to those in a thermal distribution (cf. Eqs. (6.2) and (6.3)).

---

[19] We take $\lambda = 3.4 \times 10^{-3}$, $\xi = 1500$, $g_1 = 0.44$, $g_2 = 0.53$.

[20] Indeed, for the first oscillation and typical values of the couplings in the two cases, we have $\frac{\Delta n_F^r}{\Delta n_F^t} \simeq \sqrt{\frac{\lambda_r}{\lambda_t}}\left(\frac{\xi_t}{\xi_r}\right)^2 \simeq 20.5$, $\frac{E_F^r}{E_F^t} \simeq \sqrt{\frac{\xi_t}{\xi_r}} \simeq 3.2$ and $\frac{\Delta\rho_F^r}{\Delta\rho_F^t} \simeq \sqrt{\frac{\lambda_r}{\lambda_t}}\left(\frac{\xi_t}{\xi_r}\right)^{5/2} \simeq 65$ for the first semioscillation. Combining these results with the relation between the background energy densities in the two cases, $\frac{\rho_\chi^r}{\rho_\chi^t} \simeq \frac{\lambda_r}{\lambda_t}\left(\frac{\xi_t}{\xi_r}\right)^2 \simeq 3.95$, we get $\frac{\Delta\rho_F^r}{\rho_\chi^r} \simeq 15\frac{\Delta\rho_F^t}{\rho_\chi^t}$.
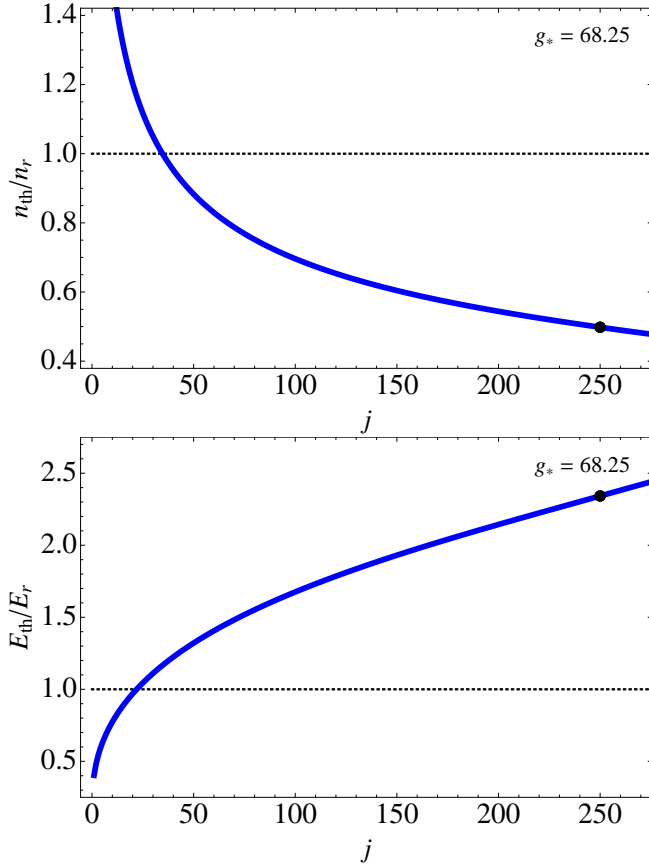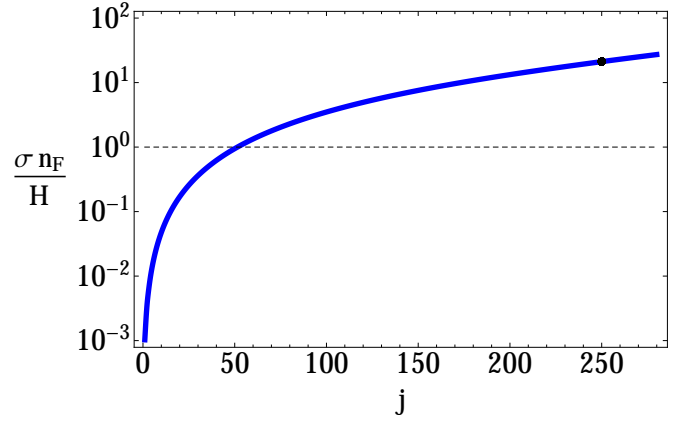
FIG. 12. Ratio between the fermion annihilation rate and the expansion rate as a function of the number of semioscillations j.

with the expansion rate. As shown in Fig. 12, the rate (6.4) exceeds the Hubble rate just a few tens of oscillations after the end of inflation. The fermions present at radiation domination ($j = j_r$) will thermalize in $t_{\rm th} \sim (\sigma n_F)^{-1}|_{j_r} \sim 0.05\, H^{-1}|_{j_r} \sim 15$ semioscillations. This allows us to interpret the radiation temperature T_r at that time as the reheating temperature T_{RH} setting the onset of the hot Big Bang. Taking into account the number of degrees of freedom after thermalization ($g_* = 106.75$), we obtain

$$T_{RH}^{NC} \simeq 1.8 \times 10^{14}\ \text{GeV}. \tag{6.5}$$

This value exceed the critical temperature T_+^{NC} needed for driving the Higgs field towards the true electroweak vacuum (cf. Eq. (5.5)). Non-critical Higgs inflation can take place even if SM vacuum is metastable.

B. Critical Higgs inflation

In critical Higgs inflation, the value of the non-minimal coupling ξ is relatively small ($\xi \sim 10$) and the jumps in the coupling constants appear closer to the Planck scale (cf. Fig. 6). As shown in Fig. 13, the energy stored in the Higgs field after inflation is *comparable* to the height of the barrier separating the two vacua. Converting the energy density of the inflaton field at the end of inflation ($V^{1/4} \simeq 6 \times 10^{16}$ GeV) into an instantaneous radiation temperature, we obtain an upper bound $T_{\rm max}^C$ on the reheating temperature[23]

$$T_{\rm RH}^C < T_{\rm max}^C = 7.85 g_*^{-1/4} \times 10^{16}\ \text{GeV}. \tag{6.6}$$

FIG. 11. Comparison between the number and average energy of fermions and those associated to a thermal distribution with temperature $T_r(j)$ and total number of degrees of freedom $g_* = 68.25$.

In the case of an overoccupied plasma, thermalization proceeds by energy cascading from the overoccupied modes with low momentum to the higher momentum modes with lower occupancy. Number changing processes $2 \leftrightarrow 1$ are expected to be parametrically as efficient as elastic scatterings or annihilations [40]. An estimate[21] of the thermalization time can be obtained by comparing the annihilation rate of fermions via electroweak interactions[22]

$$\Gamma \sim \sigma n_F \sim \frac{\alpha_W^2}{s} n_F, \tag{6.4}$$

---

[21] A proper analysis would require the use of Boltzmann equations.

[22] Here $\alpha_W \equiv g_2^2/(4\pi)$ is the electroweak coupling constant, $s \simeq (2E_F(j))^2$ stands for the square of the center-of-mass energy and n_F is the total number density of fermions. We omit factors correcting for the charge of the fermion and the number of colors. The cross section for the annihilation through a gluon can be obtained (up to color factors), by simply replacing α_W by α_s. The contribution of electroweak and QCD processes is expected to be quite similar due to the approximate unification of α_W and α_s at the preheating scale.

---

[23] A more realistic bound taking into account the particle production at the bottom of the potential is presented, for completion, in Appendix D.

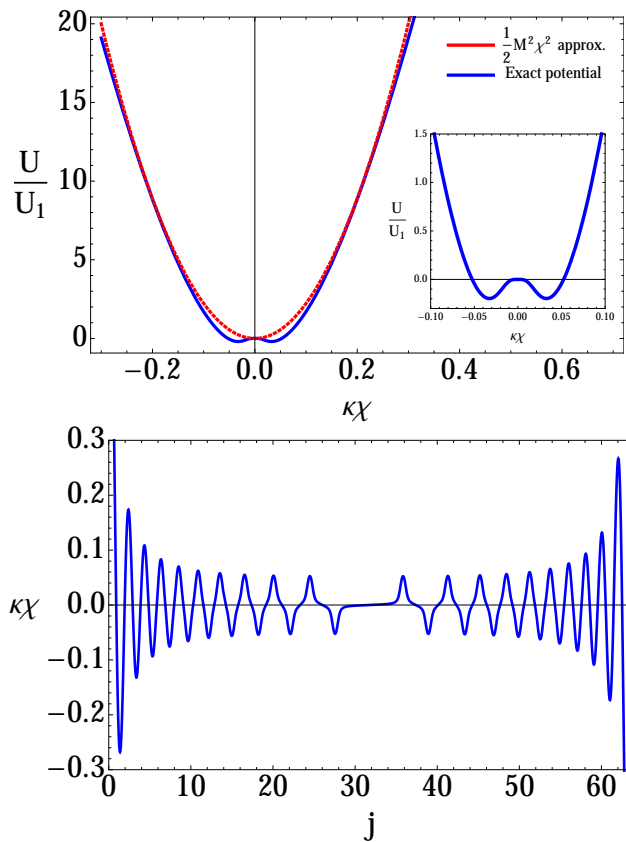FIG. 14. Scale factor as a function of the number of semioscillations j.

FIG. 13. (color online) Top: Comparison between the exact renormalization group enhanced potential and the quadratic approximation (A1) in the same regime. The normalization scale U_1 is taken to be $U_1 = 10^{-9} M_P^4$ and $\kappa = M_P^{-1}$. Bottom: Evolution of the background field χ in the critical case as a function of the number of oscillations j.

Since $T_{\rm RH}^C < T_{\rm max}^C < T_+$, the shape of the potential remains unchanged in the presence of thermal corrections and the system inevitably relax towards the minimum of the potential at Planck values. When the energy on the field becomes equal to the amplitude of the barrier ($j \simeq 30$), the expansion of the Universe stops. From there on, the scale factor begins to shrink and the amplitude of the field increases with time (cf. Fig. 13). Eventually, the kinetic energy of the Higgs field starts dominating the total energy density ($p \approx \rho$) and the Universe generated by critical Higgs inflation with metastable electroweak vacuum collapses [28], cf. Fig. 14 .

VII.   CONCLUSIONS

Although the present experimental data are perfectly consistent with the absolute stability of Standard Model within the experimental and theoretical uncertainties, one should not exclude the possibility that other experiments will be able to establish the metastability of the electroweak vacuum in the future. Should the Higgs in-
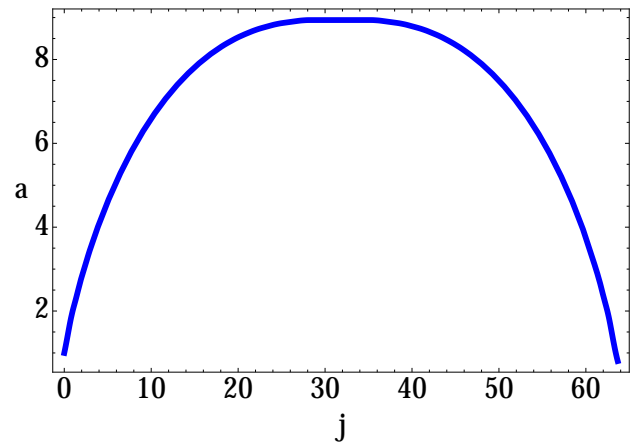
flation idea be abandoned in this case? This paper gives a negative answer to this question.

We reconsidered the validity of Higgs inflation for values of the Higgs and top quark masses giving rise to the instability of the SM vacuum at energy scales below the scale of inflation. The analysis was performed within a *self-consistent* approach based on the approximate scale invariance of the theory at large field values and on the absence of additional heavy particles between the electroweak and the Planck scale. The non-minimal coupling to gravity makes the SM non-renormalizable and requires the addition of an infinite number of counterterms. These counterterms differ from those already present in the original theory but do not modify the asymptotic properties of the model. In particular, the evolution equations for the couplings constants can be approximated by the usual SM renormalization group equations at low energies and by those of the chiral Standard Model at high energies. The ambiguities associated to the non-renormalizability of the theory appear only in the narrow interface between these two asymptotic regions and are connected to the finite parts of the counterterms. These finite parts give rise to "jumps" in the evolution of the coupling constants, whose amplitude cannot be determined within the theory itself.

As a proof of existence, we determined a set of parameters giving rise to non-critical Higgs inflation in the case of a metastable SM vacuum and studied the subsequent evolution of the Universe. Taking into account the non-perturbative production of SM particles after the end of inflation, we estimated the reheating temperature and compared it with the temperature needed to stabilize the effective potential. We showed that, while critical Higgs inflation does necessarily require the absolute stability of the SM vacuum, the successful non-critical Higgs inflation can be possible even if our vacuum is metastable.

Appendix A: Combined preheating formalism

In this appendix, we summarize the combined preheating formalism [38, 39]. Let assume the shape of the inflationary potential during the whole reheating can be well approximated by a quadratic potential[24]

$$U(\chi) \simeq \frac{1}{2}M^2\chi^2 , \qquad M = \sqrt{\frac{\lambda}{3}}\frac{M_P}{\xi} . \qquad (A1)$$

In this potential, the Universe expands as in a matter-dominated background ($a \propto t^{2/3}$) with zero pressure and energy density $\rho_\chi(t) = \frac{1}{2}M^2\chi(t)^2$. The evolution of the Higgs field is given by

$$\chi(t) = \frac{\chi_e \sin(Mt)}{Mt} = \frac{\chi_e \sin(\pi j)}{\pi j} \equiv \chi(j)\sin(\pi j) , \quad (A2)$$

with $j = Mt/\pi$ the number of semioscillations or zero crossings and $\chi_e = \sqrt{8/3}M_P$ an initial amplitude dictated by the covariant conservation law $\dot{\rho}_\chi = -3H\rho_\chi$.

The evolution equation for the gauge boson fluctuations is this background

$$\ddot{B}_k + 3H\dot{B}_k + \left(\frac{k^2}{a^2} + \tilde{m}_B^2(t)\right)B_k = 0 , \qquad (A3)$$

with $B = W, Z$ and

$$\tilde{m}_B^2(t) \equiv \frac{m_B^2}{\Omega^2} = \frac{g^2 M_P^2(1 - e^{-\sqrt{2/3}\kappa|\chi(t)|})}{4\xi} , \qquad (A4)$$

the conformally rescaled version of Jordan frame masses $m_B = gh/2$. The friction term $3H\dot{B}_k$ can be eliminated by performing a conformal redefinition of the gauge fields $(B_k \to a^{-3/2}B_k)$ to obtain[25]

$$B_k'' + \left(K^2 + \frac{\tilde{m}_B^2(t)}{M^2}\right)B_k = 0 , \qquad (A5)$$

with $K \equiv \frac{k}{aM}$ a rescaled momentum and the primes denoting derivatives with respect to a rescaled time $\tau = Mt$. Here we have adopted a compact notation in which $g = g_2, g_2/\cos\theta_W$ for the $B = W, Z$ bosons respectively, $\theta_W = \tan^{-1}(g_1/g_2)$ is the weak mixing angle and g_1 and g_2 are the gauge couplings associated to the Standard Model $U(1)_Y$ and $SU(2)_L$ gauge groups.

Particle production takes place within a very restricted field interval ($|\chi| \ll \chi_a$) around the minimum of the potential, in which the adiabaticity condition $|\dot{\tilde{m}}_B| \ll \tilde{m}_B^2$ is violated [44]. In this region, the effective square masses (A4) become linear in the field ($\tilde{m}_B^2 \propto |\chi(\tau)| \propto |\sin\tau|/j \approx |\tau|/j$) and the evolution equation (A5) can be rewritten as

$$-B_k'' - \frac{q_B}{j}|\tau|B_k = K^2 B_k , \qquad q_B \equiv \frac{g^2\xi}{\pi\lambda} . \quad (A6)$$

The previous equation can be formally interpreted as the Schrödinger equation of a particle crossing a (periodic) inverted triangular potential. To solve it, we note that the non-adiabaticity region $\chi_a = \left[\lambda\pi j/(4g^2\xi)\right]^{\frac{1}{3}}\chi(j) \simeq (10^{-6}j)^{1/3}\chi(j)$ is much smaller than the background field value $\chi(j)$ for at least hundred thousand oscillations. This justifies the use of a WKB approximation for computing the number of particles after the j-th scattering, $n_k(j^+)$, in terms of the number of particles just before that scattering, $n_k(j^-)$. After some computations, we get [45]

$$n_k(j^+) = C(x_j) + (1 + 2C(x_j))\,n_k(j^-) \qquad (A7)$$
$$+ 2\cos\theta_{j-1}\sqrt{C(x_j)\left[C(x_j)+1\right]}\sqrt{n_k^2(j^-) + n_k(j^-)} ,$$

with

$$C(x_j) \equiv \pi^2\left[\text{Ai}\left(-x_j^2\right)\text{Ai}'\left(-x_j^2\right) + \text{Bi}\left(-x_j^2\right)\text{Bi}'\left(-x_j^2\right)\right]^2 ,$$

an infrared window function depending on Airy functions of first and second type,

$$x_j \equiv \frac{K}{(q_B/j)^{1/3}} = \frac{j^{1/3}k}{Mq_B^{1/3}a_j} , \qquad (A8)$$

and $\{\theta_j\}$ some accumulated phases at each scattering. A simple estimation of these phases reveals that they are essentially incoherent ($\Delta\theta_j \sim g\,(\xi/\lambda)^{1/2}\,j^{-1/2} \sim \mathcal{O}(10^2)j^{-1/2} \gg \pi$) for the first few thousands of oscillations (cf. Ref. [38, 39] for details). This allows us to reduce (A7) to a phase-average relation [46]

$$\left(\frac{1}{2} + n_k(j^+)\right) \simeq A(x_j)\left(\frac{1}{2} + n_k(j^-)\right) , \qquad (A9)$$

with enhancing Bose factor $A(x_j) \equiv 1 + 2\text{C}(x_j)$.

Once produced, the gauge bosons tend to transfer energy into the Standard Models fermions (F) through decays ($B \to F\bar{F}$) and annihilations ($BB \to F\bar{F}$). The decay modes are expected to be the dominant processes at early times, where the number densities are still low ($\Gamma_B \gg \sigma n_B$). Let us assume that this relation holds for the typical number of semioscillations we are interested in[26]. In that case, the occupation numbers for the gauge

---

[24] As for instance happens in the non-critical case, cf. Section VI A.

[25] The redefinition introduces terms proportional to H^2 and $\ddot{a}/a$ that can be safely neglected at scales below the horizon.

[26] As we will show *a posteriori* in Appendix B, this in indeed a very good approximation.

bosons just before the j-th scattering can be written as

$$n_k(j^-) = n_k((j-1)^+) e^{-\langle \Gamma_B \rangle_{j-1} \frac{T}{2}} . \quad (A10)$$

The average $\langle \Gamma_B \rangle_j$ stands for the mean decay width of the W and Z bosons between two consecutive zero-crossings[27] [47]

$$\langle \Gamma_{W \to all} \rangle_j = \frac{3g_2^2 \langle \tilde{m}_W \rangle}{16\pi} \equiv \frac{2\gamma_W}{T} F(j) , \quad (A11)$$

$$\langle \Gamma_{Z \to all} \rangle_j = \frac{2 \text{Lips} \langle \Gamma_{W \to all} \rangle_j}{3 \cos^3 \theta_W} \equiv \frac{2\gamma_Z}{T} F(j) , \quad (A12)$$

with $\text{Lips} \equiv \frac{7}{4} - \frac{11}{3} \sin^2 \theta_W + \frac{49}{9} \sin^4 \theta_W$ a *Lorentz invariant phase-space* factor,

$$\gamma_W \equiv \frac{3g_2^3}{32} \left(\frac{3\xi}{\lambda} \right)^{1/2} , \quad \gamma_Z \equiv \frac{2 \text{Lips}}{3 \cos^3 \theta_W} \gamma_W . \quad (A13)$$

and[28]

$$F(j) \equiv \int_0^\pi \frac{dx_j}{\pi} \left(1 - e^{-\sqrt{2/3}\kappa |\chi(x_j)|} \right)^{1/2} \simeq \frac{1}{0.57 + 1.94\sqrt{j}} .$$

Combining Eqs. (A9) and (A10), we obtain [46]

$$\left(\frac{1}{2} + n_k((j+1)^+) \right) = A(x_j) \left(\frac{1}{2} + n_k(j^+) e^{-\gamma F(j)} \right) (A14)$$

The recursive iteration of this master equation allows us to obtain the total number of gauge bosons at each crossing

$$n_B(j^+) = \int \frac{k^2 n_k(j^+) dk}{2\pi^2 a_j^3} = \frac{q_B M^3}{2\pi^2 j} \int x_j^2 n_k(x_j^+) dx_j , \quad (A15)$$

and with it their total energy density[29]

$$\rho_B(j) = \rho_W(j) + \rho_Z(j) , \quad (A16)$$

$$\rho_W(j) = 2 \times 3 \, n_W(j^+) \langle m_W \rangle_j , \quad (A17)$$

$$\rho_Z(j) = 1 \times 3 \, n_Z(j^+) \langle m_Z \rangle_j . \quad (A18)$$

On the other hand, the number of fermions produced by the decay of the gauge bosons between two consecutive scatterings and their corresponding energy density are given by

$$\Delta n_F(j) \equiv \Delta n_F^{(W)}(j) + \Delta n_F^{(W)}(j) , \quad (A19)$$

$$\Delta \rho_F(j) = \Delta n_F^{(W)}(j) E_F^{(W)}(j) + \Delta n_F^{(Z)}(j) E_F^{(Z)}(j) , \quad (A20)$$

---

[27] Note that the number of W bosons surviving every semioscillation of the Higgs field is larger than the number of Z bosons ($\Gamma_W < \Gamma_Z$). The W bosons are expected to become resonant before that the Z bosons.

[28] The last equality in this equation is just a good fit for *all* j, including the first semioscillations.

[29] The factor 2 accounts for the W^+ and W^- while the factors 3 reflects the fact that each gauge boson can have one of three polarizations.

with[30]

$$\Delta n_F^{(W)}(j) = 2 \times 3 \left(2 \, n_W(j^+)(1 - e^{-\gamma_W F(j)}) \right) , \quad (A21)$$

$$\Delta n_F^{(Z)}(j) = 2 \times 3 \left(n_Z(j^+)(1 - e^{-\gamma_Z F(j)}) \right) , \quad (A22)$$

and

$$E_{F(B)}(j) \approx \frac{1}{2} \langle \tilde{m}_B \rangle_j = \frac{\sqrt{3\pi q_B}}{4} F(j) M , \quad (A23)$$

the mean energy of the relativistic decay products F of the non-relativistic gauge boson B. Summing over the number of oscillations and taking into account the dilution due to the expansion of the Universe, the total number of fermions and their total energy density after j semioscillations become

$$n_F(j) = \sum_{i=1}^{j} \left(\frac{i}{j} \right)^2 \Delta n_F(i) , \quad (A24)$$

$$\rho_F(j) = \sum_{i=1}^{j} \left(\frac{i}{j} \right)^{8/3} \Delta \rho_F(i) , \quad (A25)$$

Appendix B: Consistency checks

The combined preheating formalism presented in the previous section assumes that:

i. The frequency M used to describe the background evolution in (A5) is not significantly modified by particle production.

ii. The condition $\Gamma_B \gg \sigma n_B$ holds during the whole preheating process.

To verify the consistency of the approach, we perform two consistency checks:

i. We use the number densities obtained through the combined preheating formalism to estimate the back-reaction on M. The effective frequency is given by $\omega^2 \approx M^2 \left[1 + \Delta M_{BR}^B + \Delta M_{BR}^F \right]$, with

$$\Delta M_{BR}^B \equiv \frac{g\sqrt{\lambda} n_B(j)}{6^{3/4}} \left(\frac{\pi j}{\xi} \right)^{3/2} , \quad (B1)$$

$$\Delta M_{BR}^F \equiv \frac{y_f \sqrt{\lambda} n_B(j)}{\sqrt{2} \, 6^{3/4}} \left(\frac{\pi j}{\xi} \right)^{3/2} \quad (B2)$$

the contribution of the created gauge bosons and fermions [38].

As shown in Fig. 15, ΔM_{BR}^B and ΔM_{BR}^F turn out completely negligible at all times before the onset of radiation domination, which justifies the use of Eq. (A7).

---

[30] The factor 2 accounts for the fact that each gauge boson decays into two fermions.
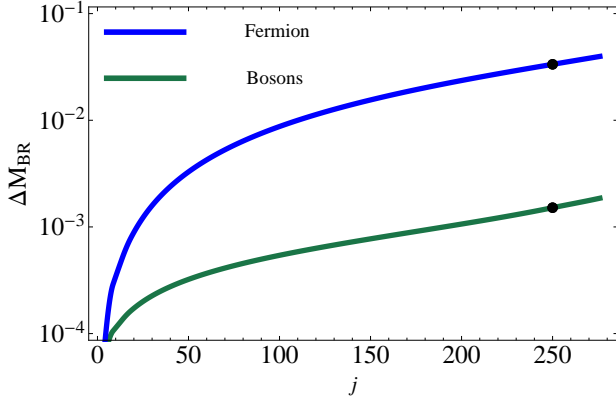
FIG. 15. (color online) Contribution of the created gauge bosons and fermions to the background frequency M as a function of the number of oscillations.
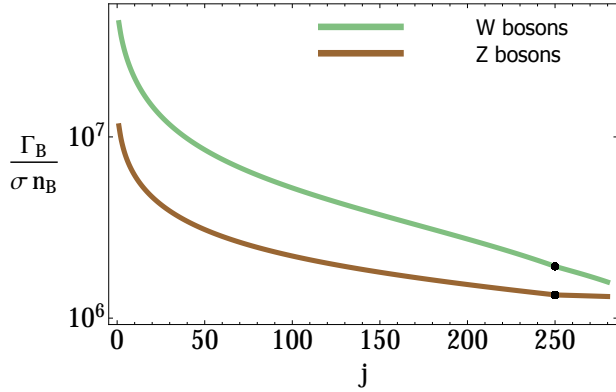

FIG. 16. (color online) Comparison between the decay channels $B \to F\bar{F}$ and the scattering channel $WW \to F\bar{F}$.

ii. We verify a posteriori the assumption $\Gamma_B \gg \sigma n_B$. The result showed in Fig. 16 justifies the use of Eq. (A10).

Appendix C: Non-perturbative Higgs production in non-critical case

In this appendix we derive an upper bound for the non-perturbative production of Higgs particles in non-critical Higgs inflation. In Fourier space, the Einstein-frame equation of motion for these perturbations reads

$$\delta\chi_k''(t) + \left(K^2 + \frac{V_{,\chi\chi}}{M^2}\right)\delta\chi_k(t) = 0, \qquad \text{(C1)}$$

with $K \equiv \frac{k}{aM}$ a rescaled momentum and the primes denoting derivatives with respect to a rescaled time $\tau = Mt$.

A simple inspection of the potential in Fig. 9 suggests that the leading contribution to Higgs production should be associated to the region $|\chi| \leq \chi_T$ in which the curvature of the potential ($V_{,\chi\chi}$) becomes negative [48]. Let

us assume for simplicity that this curvature is constant. Denoting it by $-M_T^2$, we can rewrite Eq. (C1) as

$$\delta\chi_k''(t) - \Omega_T^2\delta\chi_k(t) = 0, \qquad \Omega_T^2 \equiv q_T^2 - K^2, \quad \text{(C2)}$$

with $q_T^2 \equiv M_T^2/M^2 \approx 0.067$ the numerical value of M_T^2 in units of the curvature of the potential at large field values. The amplification of modes with $K < q_T$ is given by

$$\Delta\delta\chi_k^j \sim \exp\left(\Omega_T M \Delta t_j\right), \qquad \text{(C3)}$$

with Δt_j denoting the time expended by the background Higgs field in the tachyonic region $|\chi| \leq \chi_T$ for a given semioscillation j. Estimating this time via Eq. (A2)

$$M\Delta t \approx \frac{2\pi\chi_T}{\chi_e}\frac{1}{j}, \qquad \text{(C4)}$$

we can rewrite Eq. (C3) as

$$\Delta\delta\chi_k^j \sim e^{A(j)j}, \qquad A(j) \equiv \frac{2\pi\chi_T\Omega_T(j)}{\chi_e} \qquad \text{(C5)}$$

The total amplification after a given number of oscillations will be the result of the interference of the individual amplifications (C5). Since we are just seeking for an upper bound on Higgs production, we will assume that the interference is fully constructive and that all the modes within the band $K < q_T$ grow at the maximum possible rate (i.e at the rate of the zero mode, $k = 0$).

$$A \approx \frac{2\pi\chi_T q_T}{\chi_e} \qquad \text{(C6)}$$

With these two assumptions, the occupation number of a given mode k after j semioscillations becomes

$$n_k^j \sim \prod_j (\Delta\delta\chi_k^j)^2 \simeq \exp\left(2A\sum_j j\right) \simeq e^{Aj^2} \quad \text{(C7)}$$

where in the last step we have assumed a large number of semioscillations and approximated $\sum_j j = 1/2j(j+1) \simeq j^2/2$.

The total number of Higgs particles at their associated energy density after j semioscillations is obtained by integrating over all the amplified modes $K < q_T$ (i.e, over $k < aM_T$). Taking into account that $a = j^{2/3}$, we obtain

$$n_{\delta\chi}(j) = \frac{1}{2\pi^2 a^3}\int_0^{aM_T} dk\, k^2\, n_k \simeq \frac{q_T^3 M^3}{6\pi^2}e^{Aj^2} \qquad \text{(C8)}$$

$$\rho_{\delta\chi}(j) = \frac{1}{2\pi^2 a^3}\int_0^{aM_T} dk\, k^2\, |\Omega_k| n_k \simeq \frac{q_T^4 M^4}{6\pi^2}e^{Aj^2} \quad \text{(C9)}$$

Evaluating (C9) at the time in which the energy density of fermions starts dominating the expansion of the Universe ($j^* = 250$), we get

$$\rho_{\delta\chi}(j^*) \simeq 10^{-4}\rho_F(j^*), \qquad \text{(C10)}$$

The contribution of Higgs particle production in non-critical Higgs inflation is completely negligible even with the extreme approximations performed in this appendix (namely constructive interference and maximum growing for all the modes.).
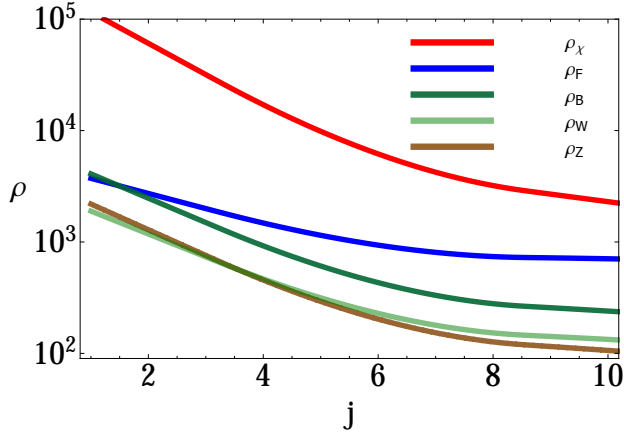
FIG. 17. (color online) Evolution of the different energy densities (in M^4 units) for the critical case ($\lambda = 3 \times 10^{-4}$, $\xi = 15$, $g_1 = 0.44$, $g_2 = 0.53$). The shaded region indicates the limit of applicability of the combined preheating formalism as formulated in Appendix A
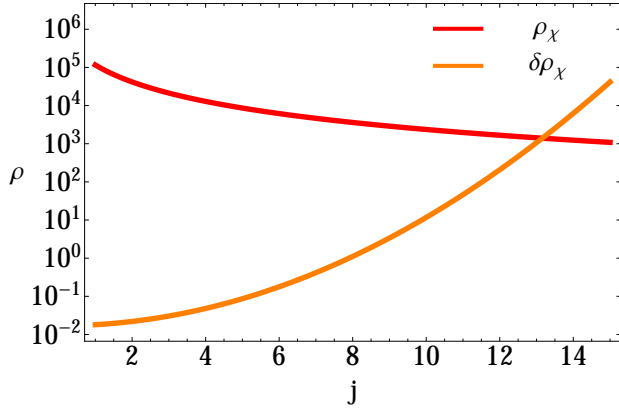

FIG. 18. (color online) Comparison between the energy density of the background and that into Higgs particles (both in M^4 units) as a function of the number of semioscillations.

Appendix D: Non-perturbative particle production in the critical case

A proper treatment of particle creation in critical Higgs inflation would require the join analysis of combined preheating and the tachyonic Higgs particle production at the bottom of the potential. Here we will simply try to derive some estimates on the separated processes. We start by applying the combined preheating formalism to the first few oscillations ($j < 10$) in which the quadratic approximation (A1) still holds. The resulting evolution of the different energy densities[31] is shown in Fig. 17. As in the non-critical case, the creation of particles is not ef-

ficient enough to dominate the expansion of Universe in such a short period of time. Although the features of the potential could change the pattern of particle creation at later times, the energy density into fermions will never exceed[32] the energy of the Higgs field at $j \simeq 10$.

The production of Higgs particles by tachyonic instability can be estimated along the lines presented in Appendix C. In order to obtain a conservative bound for the maximum reheating temperature, we will assume that the interference between the different scattering is maximally constructive and that all the tachyonic modes grow at the maximum rate (i.e that the zero mode $k = 0$). As shown in Fig. 18, the energy density into Higgs particles equals the energy into the background field in just $j \simeq 13$ semioscillations. The tachyonic production becomes the leading mechanism for particle creation in the non-critical case[33]. Transforming this energy into the instantaneous radiation temperature of a plasma containing $g_* = 68.25$ degrees of freedom, we obtain an upper bound for the reheating temperature in the critical case, namely

$$T_{\mathrm{RH}}^C < 5 \times 10^{15}\,\mathrm{GeV}\,. \tag{D1}$$

This temperature is smaller than the restoration temperature T_+, the shape of the potential remains unchanged and the system eventually finishes in the wrong minimum at large field values.

----

[31] To avoid misunderstandings, we emphasize that the unit M is computed with the values of ξ and λ associated to the critical case.

[32] The quantity ρ_χ traces the maximum (total) energy of the system (it takes into account the expansion of the Universe but not the decay due to particle creation).

[33] Contrary to the non-critical case, the region in which the effective mass of the Higgs (i.e. $V_{\chi\chi}$) becomes negative is quite large ($\Delta\chi \sim \mathcal{O}(10^{-2})M_P$)

[1] G. Aad *et al.* [ATLAS Collaboration], Phys. Lett. B **716** (2012) 1 [arXiv:1207.7214 [hep-ex]].

[2] S. Chatrchyan *et al.* [CMS Collaboration], Phys. Lett. B **716** (2012) 30 [arXiv:1207.72 35 [hep-ex]].

[3] F. Bezrukov, M. Y. Kalmykov, B. A. Kniehl and M. Shaposhnikov, JHEP **1210** (2012) 140 [arXiv:1205.2893 [hep-ph]].

[4] G. Degrassi, S. Di Vita, J. Elias-Miro, J. R. Espinosa, G. F. Giudice, G. Isidori and A. Strumia, JHEP **1208** (2012) 098 [arXiv:1205.6497 [hep-ph]].

[5] D. Buttazzo, G. Degrassi, P. P. Giardino, G. F. Giudice, F. Sala, A. Salvio and A. Strumia, JHEP **1312** (2013) 089 [arXiv:1307.3536 [hep-ph]].

[6] F. Bezrukov and M. Shaposhnikov, arXiv:1411.1923 [hep-ph].

[7] V. Branchina and E. Messina, Phys. Rev. Lett. **111** (2013) 241801 [arXiv:1307.5193 [hep-ph]].

[8] V. Branchina, E. Messina and A. Platania, JHEP **1409** (2014) 182 [arXiv:1407.4112 [hep-ph]].

[9] V. Branchina, E. Messina and M. Sher, arXiv:1408.5302 [hep-ph].

[10] F. L. Bezrukov and M. Shaposhnikov, Phys. Lett. B **659** (2008) 703 [arXiv:0710.3755 [hep-th]].

[11] https://cds.cern.ch/record/1951019?ln=en

[12] [ATLAS and CDF and CMS and D0 Collaborations], arXiv:1403.4427 [hep-ex].

[13] Tevatron Electroweak Working Group [CDF and D0 Collaborations], arXiv:1407.2682 [hep-ex].

[14] F. Bezrukov, A. Magnin, M. Shaposhnikov and S. Sibiryakov, JHEP **1101** (2011) 016 [arXiv:1008.5157 [hep-ph]].

[15] F. Bezrukov and M. Shaposhnikov, Phys. Lett. B **734** (2014) 249 [arXiv:1403.6078 [hep-ph]].

[16] C. P. Burgess, H. M. Lee and M. Trott, JHEP **0909** (2009) 103 [arXiv:0902.4465 [hep-ph]].

[17] J. L. F. Barbon and J. R. Espinosa, Phys. Rev. D **79** (2009) 081302 [arXiv:0903.0355 [hep-ph]].

[18] C. P. Burgess, H. M. Lee and M. Trott, JHEP **1007** (2010) 007 [arXiv:1002.2730 [hep-ph]].

[19] S. Ferrara, R. Kallosh, A. Linde, A. Marrani and A. Van Proeyen, Phys. Rev. D **83** (2011) 025008 [arXiv:1008.2942 [hep-th]].

[20] F. Bezrukov and M. Shaposhnikov, JHEP **0907** (2009) 089 [arXiv:0904.1537 [hep-ph]].

[21] A. O. Barvinsky, A. Y. Kamenshchik and A. A. Starobinsky, JCAP **0811** (2008) 021 [arXiv:0809.2104 [hep-ph]].

[22] A. De Simone, M. P. Hertzberg and F. Wilczek, Phys. Lett. B **678** (2009) 1 [arXiv:0812.4946 [hep-ph]].

[23] A. O. Barvinsky, A. Y. Kamenshchik, C. Kiefer, A. A. Starobinsky and C. Steinwachs, JCAP **0912** (2009) 003 [arXiv:0904.1698 [hep-ph]].

[24] A. O. Barvinsky, A. Y. Kamenshchik, C. Kiefer, A. A. Starobinsky and C. F. Steinwachs, Eur. Phys. J. C **72** (2012) 2219 [arXiv:0910.1041 [hep-ph]].

[25] Y. Hamada, H. Kawai, K. y. Oda and S. C. Park, Phys. Rev. Lett. **112** (2014) 241301 [arXiv:1403.5043 [hep-ph]].

[26] A. C. Longhitano, Phys. Rev. D **22** (1980) 1166.

[27] A. D. Linde, Contemp. Concepts Phys. **5** (1990) 1 [hep-th/0503203].

[28] G. N. Felder, A. V. Frolov, L. Kofman and A. D. Linde, Phys. Rev. D **66** (2002) 023507 [hep-th/0202017].

[29] A. D. Linde, Rept. Prog. Phys. **42** (1979) 389.

[30] K. Kajantie, M. Laine, K. Rummukainen and M. E. Shaposhnikov, Nucl. Phys. B **458** (1996) 90 [hep-ph/9508379].

[31] G. W. Anderson, Phys. Lett. B **243** (1990) 265.

[32] P. B. Arnold and S. Vokos, Phys. Rev. D **44** (1991) 3620.

[33] J. R. Espinosa and M. Quiros, Phys. Lett. B **353** (1995) 257 [hep-ph/9504241].

[34] J. R. Espinosa, G. F. Giudice and A. Riotto, JCAP **0805** (2008) 002 [arXiv:0710.2484 [hep-ph]].

[35] I. I. Tkachev, Phys. Lett. B **376** (1996) 35 [hep-th/9510146].

[36] R. Allahverdi, R. Brandenberger, F. Y. Cyr-Racine and A. Mazumdar, Ann. Rev. Nucl. Part. Sci. **60** (2010) 27 [arXiv:1001.2600 [hep-th]].

[37] M. A. Amin, M. P. Hertzberg, D. I. Kaiser and J. Karouby, arXiv:1410.3808 [hep-ph].

[38] J. Garcia-Bellido, D. G. Figueroa and J. Rubio, Phys. Rev. D **79** (2009) 063531 [arXiv:0812.4624 [hep-ph]].

[39] F. Bezrukov, D. Gorbunov and M. Shaposhnikov, JCAP **0906** (2009) 029 [arXiv:0812.3622 [hep-ph]].

[40] A. Kurkela and G. D. Moore, JHEP **1112** (2011) 044 [arXiv:1107.5050 [hep-ph]].

[41] K. Enqvist and K. J. Eskola, Mod. Phys. Lett. A **5** (1990) 1919.

[42] S. Davidson and S. Sarkar, JHEP **0011** (2000) 012 [hep-ph/0009078].

[43] A. Mazumdar and B. Zaldivar, Nucl. Phys. B **886** (2014) 312 [arXiv:1310.5143 [hep-ph]].

[44] L. Kofman, A. D. Linde and A. A. Starobinsky, Phys. Rev. D **56** (1997) 3258 [hep-ph/9704452].

[45] A. Galindo and P.Pascual, "Mecánica cuántica", Ed. Alhambra Universidad, Madrid (1978).

[46] D. G. Figueroa, AIP Conf. Proc. **1241** (2010) 578 [arXiv:0911.1465 [hep-ph]].

[47] Ta-Pei Cheng and Ling-Fong Li, "Gauge theory of elementary particle physics" (Oxford. U. P., UK, 2006).

[48] G. N. Felder, J. Garcia-Bellido, P. B. Greene, L. Kofman, A. D. Linde and I. Tkachev, Phys. Rev. Lett. **87** (2001) 011601 [hep-ph/0012142].